JOURNAL OF MATERIALS SCIENCE 37 (2002) 3657–3665

# Characterization of interfacial and mechanical properties of "green" composites with soy protein isolate and ramie fiber

PREETI LODHA, ANIL N. NETRAVALI
*Fiber science Program, Cornell University, Ithaca, NY 14853-4401, USA*
*E-mail: ANN2@cornell.edu*

Environment-friendly fiber-reinforced composites were fabricated using ramie fibers and soy protein isolate (SPI) and were characterized for their interfacial and mechanical properties. Ramie fibers were characterized for their tensile properties and the parameters for the Weibull distribution were estimated. Effect of glycerol content on the tensile properties of SPI was studied. Interfacial shear strength (IFSS) was determined using the microbond technique. Based on the IFSS results and fiber strength distribution, three different fiber lengths and fiber weight contents (FWC) were chosen to fabricate short fiber-reinforced composites. The results indicate that the fracture stress increases with increase in fiber length and fiber weight content. Glycerol was found to increase the fracture strain and reduce the resin fracture stress and modulus as a result of plasticization. For 10% (w/w) of 5 mm long fibers, no significant reinforcement effect was observed. In fact the short fibers acted as flaws and led to reduction in the tensile properties. On further increasing the fiber length and FWC, a significant increase in the Young's modulus and fracture stress and decrease in fracture strain was observed as the fibers started to control the tensile properties of the composites. The experimental data were compared to the theoretical predictions made using Zweben's model. The experimental results are lower than the predicted values for a variety of reasons. However, the two values get closer with increasing fiber length and FWC. 

## 1. Introduction

Fiber-reinforced composites have become increasingly popular in a variety of applications such as aerospace structures, automotive parts, building materials and sporting goods because of their high specific strength and modulus compared to the conventional metals. With the usage of these composites recording double-digit growth worldwide, their disposal after intended use is expected to become critical in the near future. As a result, there has been growing interest to develop "Green" composites using plant-based natural fibers as the reinforcement and biodegradable resin [1–6].

While the plant-based fibers may not be as strong as graphite and aramids such as Kevlar®, their main advantages are their low cost, biodegradability and yearly replenishability. The hollow tubular (cellular) structure of the plant fibers also provides excellent insulation against heat and noise for automobile applications [1]. Mohanty *et al.* [2] have provided an overview of various fully and semi-biodegradable composites [3–5]. Recently, some fully degradable green composites have also been developed, mostly using thermoplastic resins such as poly(hydroxybutyrate-co-valerate) resin (Biopol®) and polyester amides [6–9]. Wool *et al.* [10] have chemically modified the oils from soybeans for use as resins. Otaigbe *et al.* [11], Paetau *et al.* [12], Thames and Zhou [13], Liang *et al.* [14] and Lodha and Netravali [15, 16] have used soy protein as resin to make green composites.

This paper presents the processing of green composites using ramie fiber and soy protein. Soybeans, obtained from an annual plant, *Glycine max (L.) Merrill* [17], typically contain 20% oil and up to 50% protein. This protein consists of polypeptide chains of various lengths of which about 62% are polar and reactive amino acid residues. Two main varieties of soybean protein, soy protein isolate (SPI) containing 90% protein and soy protein concentrate (SPC) containing 50–70% protein, are available in the market [17].

The soy proteins (7 S and 11 S, S = svedburg unit) crosslink through covalent sulphur crosslinks under oxidative conditions at cysteine residues [18]. Dehydroalanine (DHA), formed from alanine by loss of side chain beyond the $\beta$-carbon atom, also react with lysine and cysteine to form lysinoalanine and lanthionine crosslinks, respectively [18, 19]. Besides, asparagine and lysine can also react together to form an amide-type of crosslink. All these reactions occur during the curing process of the SPI-polymer forming a resin of moderate strength [15, 16]. The SPI-polymer is highly hygroscopic/moisture sensitive in nature due to presence of amine, amide, carboxyl and hydroxyl groups [19].

Ramie fibers are obtained from the bast/stem of the annual shrub, *Boehmeria nivea* from the nettle family, Utricaceae [20, 21]. They are resistant to many chemicals, show continuous reduction in diameter at the two ends and have branches along the length.

A review article by Herrera-Franco and Drzal [22] discusses various state-of-the-art interfacial shear strength (IFSS) measurement techniques including microbond, single fiber fragmentation (single fiber composite), single fiber pull out and micro-indentation. Single fiber composite test analysis has been done using optical or acoustic emission on various fiber/resin systems [23, 24]. The single fiber pull out technique (from resin clock, disc or droplet) is believed to possess some of the characteristics of the actual fiber pull out in composites [7, 25–28]. The microbond (microbead) technique, a modification of the fiber pull out technique, has been used in many interface studies [7, 26–29]. This was the only technique found useful in the present work for estimating the IFSS.

## 2. Experimental procedures

### 2.1. Materials

Soy protein isolate (SPI) powder, PRO FAM® 970, was obtained from Archer Daniels Midland Co., IL. Unbleached (brownish) ramie fibers were supplied in a roving form by Danforth International Trade Associates Inc., NJ, USA. Analytical grade glycerol ($C_3H_5(OH)_3$), was supplied by Aldrich Inc., MO.

### 2.2. Fiber characterization

The diameters of 150 ramie fibers, conditioned at ASTM conditions (21°C and 65% R.H.) for 48 hrs, were measured using vibroscope technique as per the ASTM D 1577-90 procedure. Tensile properties of ramie fibers were characterized using Instron tensile testing machine (Instron), model 1122, according to modified ASTM D 3822-91 procedure. The tensile tests were performed at a gauge length of 50 mm and a strain rate of 0.2 $\text{min}^{-1}$. Various properties such as Young's modulus, fracture stress, fracture strain and energy to break were calculated. The fracture stress data were fit to a two parameter Weibull distribution as shown in Equation 1 and the shape parameter, $r$, scale parameter, $X_0$, and mean fracture stress, $\mu$, were determined

$$W(X) = 1 - \exp\left[-\left(\frac{X}{X_0}\right)^r\right] \tag{1}$$

$$\mu = X_0 \times \Gamma\left(1 + \frac{1}{r}\right) \tag{2}$$

where $W(X)$ is the probability for the fiber fracture stress to be less than $X$.

The surface topography of the ramie fibers was observed using an Electroscan E-3 Scanning Electron Microscope (SEM) available at the Cornell Center for Materials Research (CCMR) at Cornell University, NY.

### 2.3. Curing process for SPI

The curing method for SPI, recommended by Liang *et al.* [14], was used, with some modifications, for the current study. To prepare specimens SPI-powder was mixed with glycerol (30%, w/w) and distilled water (300%, w/w) and rolled into small balls of 40 gm each, which were hot pressed at 75°C into a circular, 1.5–2 mm thick sheet between two stainless steel plates. To enhance uniformity, each sheet, was four folded before precuring at 75°C for 30 min in the hot press and dried in air for 24 hrs. The dried sheet was hot pressed at 80°C (showed lowest viscosity) for 5 min. The specimens were repeatedly pressurized (to 0.3 MPa and at 80°C) and depressurized in order to eliminate the voids and air bubbles. Finally, the sheet was hot pressed (cured) at 110°C for 2 hrs at a pressure of 2.87–3.83 MPa. The cured SPI-polymer sheet (1 mm thick) was then conditioned for 48 hrs before testing.

### 2.4. Effect of glycerol content

The SPI-powder was mixed with 20%, 30%, 40% and 50% (w/w) of glycerol, maintaining the water at 300% (w/w of SPI) and cured using the curing cycle described in the earlier section. The specimens of 70 mm × 10 mm dimensions were tested on Instron according to ASTM D 3039-89 procedure at a gauge length of 50 mm and strain rate of 0.2 $\text{min}^{-1}$. Optimum amount of glycerol of 30%, based on mechanical properties and processibility, was used for further experiments.

### 2.5. IFSS characterization

SPI-powder with 300% water content and glycerol had high viscosity and was found to be unsuitable for forming microbeads for interfacial shear strength (IFSS) tests. Hence, the SPI-powder was mixed with 30% glycerol and 700% water compared to 300% water. This formulation resulted in the desired size of the microbeads suitable for IFSS tests. A polyethylene filament was used to transfer the resin mixture to the ramie fiber, mounted on a paper tab. The microbeads were then dried and cured using the standard thermal cycle except that no pressure was applied at any stage during curing. As the water evaporated the microbead diameter decreased to approximately half of the original size.

The fiber diameter and embeddment length were measured using a Leitz Wetzlar optical microscope at the two ends of each microbead. The IFSS test was conducted by keeping the microbead under the microvise plates and pulling the fiber on the Instron at a crosshead speed of 5 mm/min until debonding occurred. Detailed description of the microbead test can be found elsewhere [7, 26–28]. Average IFSS was calculated by dividing the debonding force by the interface area. The critical length, $l_c$, was calculated using the average IFSS value and fiber fracture stress value as shown by the Equation 3. The minimum length of the fiber, required to effectively transfer full load in the axial direction in a composite, is called the critical, load transfer or the ineffective length

$$l_c = \frac{\sigma_f \times d}{2 \times \tau} \tag{3}$$

where $\sigma_f$ is the fracture stress of the ramie fiber of length equal to $l_c$, $d$ is the fiber diameter, assuming it to be round, and $\tau$ is the average IFSS value [21].

### 2.6. Preparation of short fiber-reinforced composites

The critical length was calculated to be 2.5 mm and based on this result, three fiber lengths of 5, 10 and 15 mm were chosen. Composites with 10, 20 and 30% fiber weight contents (FWC) were prepared for all three fiber lengths used. The FWC is w/w of SPI-powder + fiber weight for the rest of the paper. Fibers of required lengths were chopped using a shear cutter. To prepare resin/fiber mixture, the SPI was mixed with 30% glycerol (w/w of SPI-powder weight) and 300% (w/w of SPI-powder + fiber weight) water and stirred to make uniform dough. To prepare composites with 10% fibers of various lengths, required amounts of SPI-powder, glycerol and water were mixed to form dough. Measured weight of chopped fibers, mixed using a compressed air canister, were slowly added to the dough by dabbing to maintain uniform distribution. The dough was made into a ball and subjected to the same curing cycle used for making SPI sheets. For composites with 20 and 30% FWC of all three lengths, required amount of SPI-powder, glycerol, water and the fibers were weighed and mixed as explained earlier. The cured composite sheets were then conditioned at ASTM conditions for 48 hrs prior to testing.

### 2.7. SPI resin and composite characterization

The SPI-polymer resin and composites was cut into specimens of 70 mm length and tested on Instron according to ASTM D 3039-89 procedure at a gauge length of 50 mm and strain rate of 0.2 $min^{-1}$. The widths of the pure resin and the composite specimens were 10 mm and twice the length of the fiber, respectively. The density of the SPI-polymer resin was measured using the density gradient column at TRI-Princeton, Princeton, NJ. The fractured surfaces of the composite were characterized using the SEM.

## 3. Results and discussion

### 3.1. Fiber characterization

The structure of the ramie fiber is cellular with cell lengths in the range of 154 mm, spiral angle of 7.5° and length-to-diameter (aspect) ratio of the cell being approximately 3500 [30]. Density of ramie fibers has been reported to be 1.5 gm/cc [20]. Ramie fibers used in this study had a length of 12 cm and an average diameter of 48.5 $\mu$m (7.8 $\mu$m). The fibers had an average fracture stress of 621 MPa (296 MPa), fracture strain of 1.9% (0.45%), Young's modulus of 47.5 GPa (15.2 GPa) and energy at break of $7.44 \times 10^{-4}$ J. The numbers in parentheses are the standard deviation values. The scale and shape parameters were calculated to be 710 MPa and 2.6, respectively. It is clear from these data that the fiber mechanical properties have large variability which is common for all natural fibers. Figs 1 and 2 show the SEM photomicrographs of the longitudinal view of the ramie fiber and an end of a ramie fiber fractured under tensile load, respectively. Fig. 1 clearly shows the fibrillar structure and the non-circular cross-section of the fiber due to the fibrils and the presence of lignin on the surface. Fig. 2 shows the separated fibrils after the tension test. On a closer view, the individual fibrils appear to have a smooth surface.

### 3.2. Effect of glycerol on the tensile properties of SPI-polymer sheet

The effect of glycerol content on various tensile properties of SPI-polymer is shown in Fig. 3. As expected, due to plasticization, the fracture strain of the pure SPI-polymer resin increased from 32% to 147% on increasing the glycerol percentage from 20% to 50%,

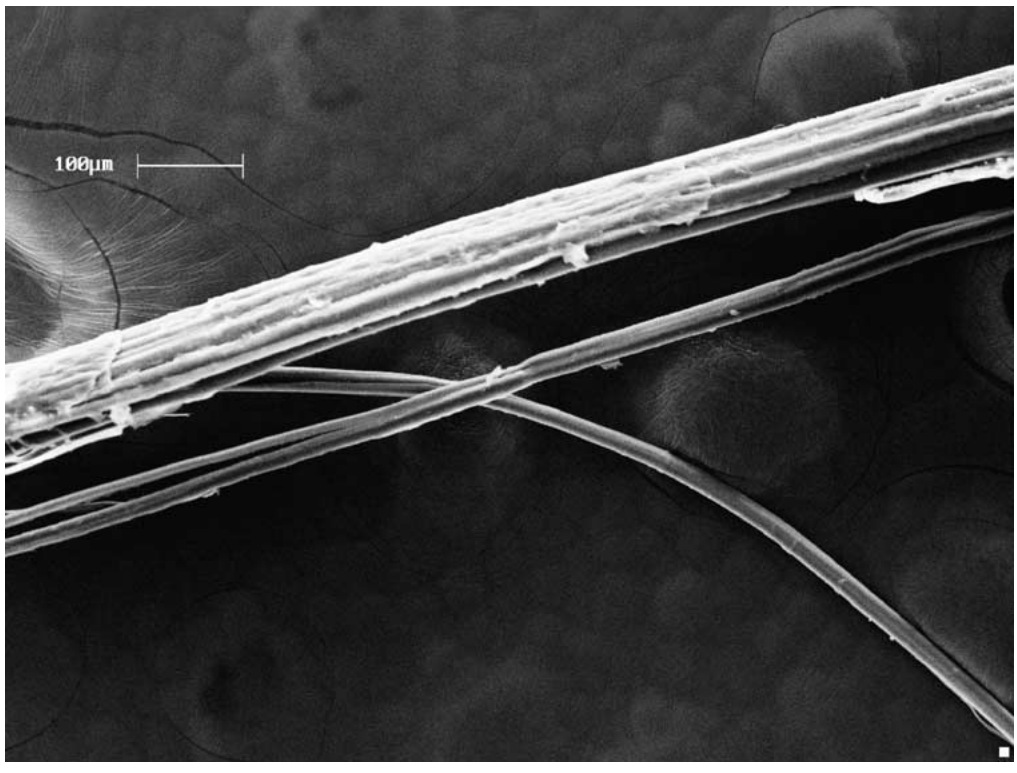


*Figure 1* SEM photomicrograph of a ramie fiber.

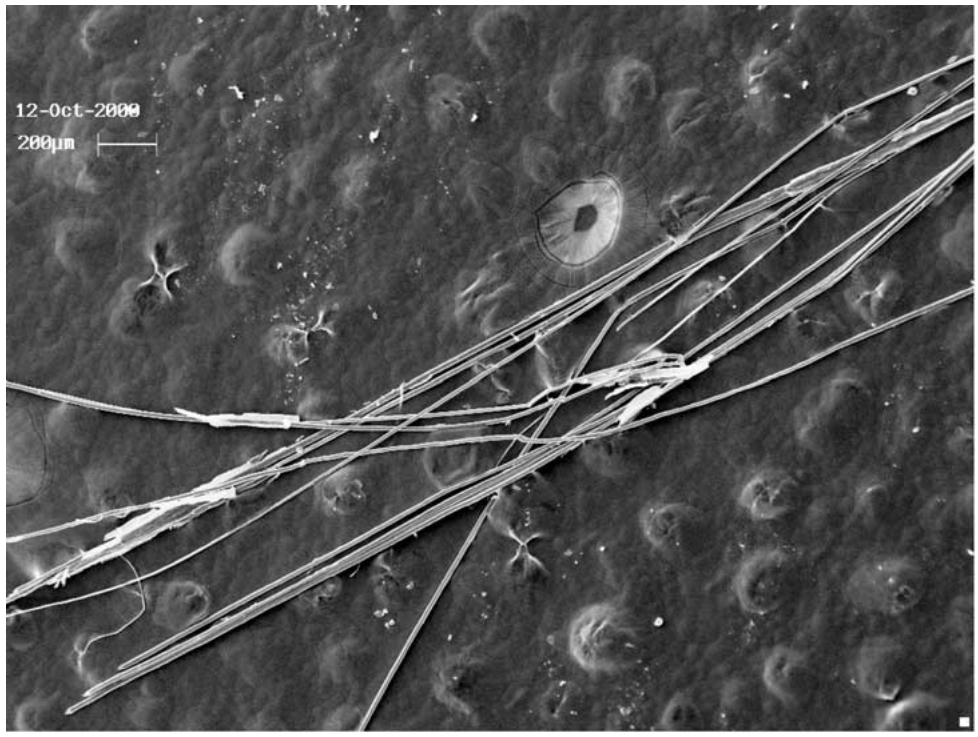


*Figure 2* SEM photomicrograph of the end of a ramie fiber fractured under tensile load.

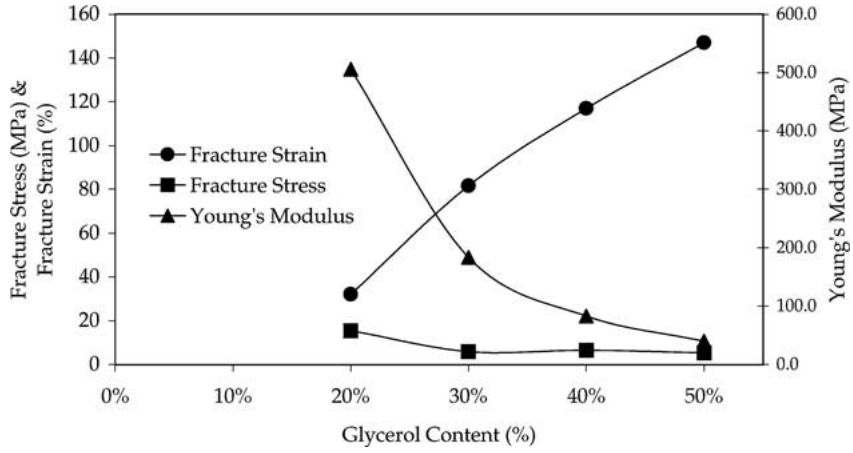


*Figure 3* Effect of glycerol content on various tensile properties of the SPI-polymer resin.

respectively. For the same reason, the Young's modulus and fracture stress values of the SPI-polymer resin decreased from 505 MPa to 40 MPa and 15.5 MPa to 5.3 MPa, respectively. The density of the SPI-polymer resin with 30% glycerol was measured to be 1.31 g/cc using a density gradient column.

Glycerol acts as a plasticizer without forming any covalent linkages with the SPI-polymer. However, due to three hydroxyl groups present in glycerol, it is expected to strongly hydrogen bond with the protein molecules at amine, amide, carboxyl and hydroxyl sites. Being small in size, it effectively increases the free volume of the system, thus decreasing the glass transition temperature. As a result, the SPI-polymer resin changes from brittle to leathery to rubbery at room temperature, as the percentage of glycerol is increased from 0% to 50%.

## 3.3. IFSS characterization

Fig. 4 shows a typical SEM photomicrograph of a SPI-polymer microbead on a ramie fiber. It can be seen that the bead is globular rather than smooth, which is characteristic of the way SPI-polymer resin dries. In addition, as mentioned earlier, the bead diameter decreases to approximately half its original size after drying. This is an inherent problem of the SPI-polymer resin system. The tested specimens showed traces of resin adhering to the fiber indicating good interface as shown in Fig. 5. The average IFSS value was calculated to be 29.8 MPa. Based on this value, the critical length was estimated to be 2.54 mm using Equation 3. The ramie fiber with a different resin (epoxy resin) has been reported to show a much higher average IFSS value of 79 MPa [19, 20]. However, in the case of epoxy, the IFSS value was characterized using a single fiber composite test and also the epoxy used was a high functionality resin creating a larger number of hydroxyl groups. Although SPI-polymer resin contains several amino acids with polar groups, it also contains amino acids such as alanine, glycine, leucine, isoleucine etc. that have non-polar groups that cannot hydrogen bond with the cellulose molecules in the fiber. Assumption of round cross-section may also add to the error in the IFSS value.

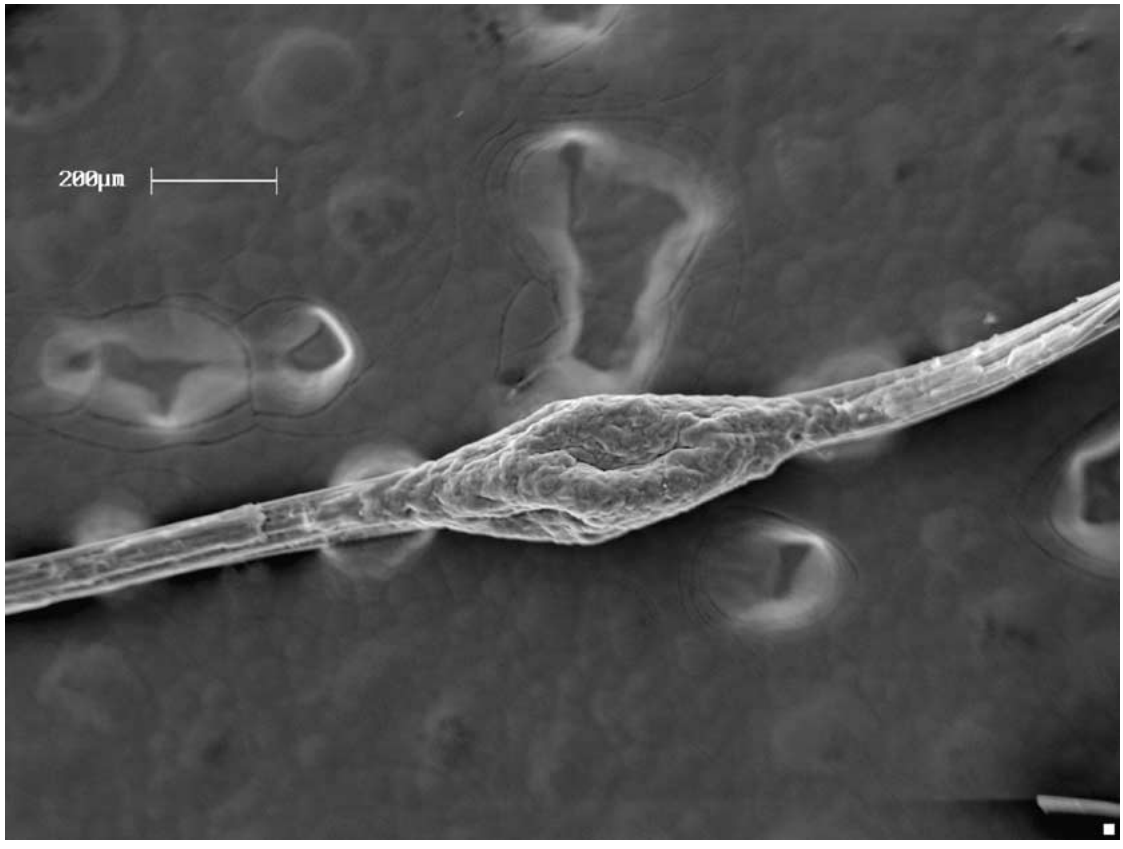


*Figure 4* SEM photomicrograph of a typical microbead on ramie fiber.

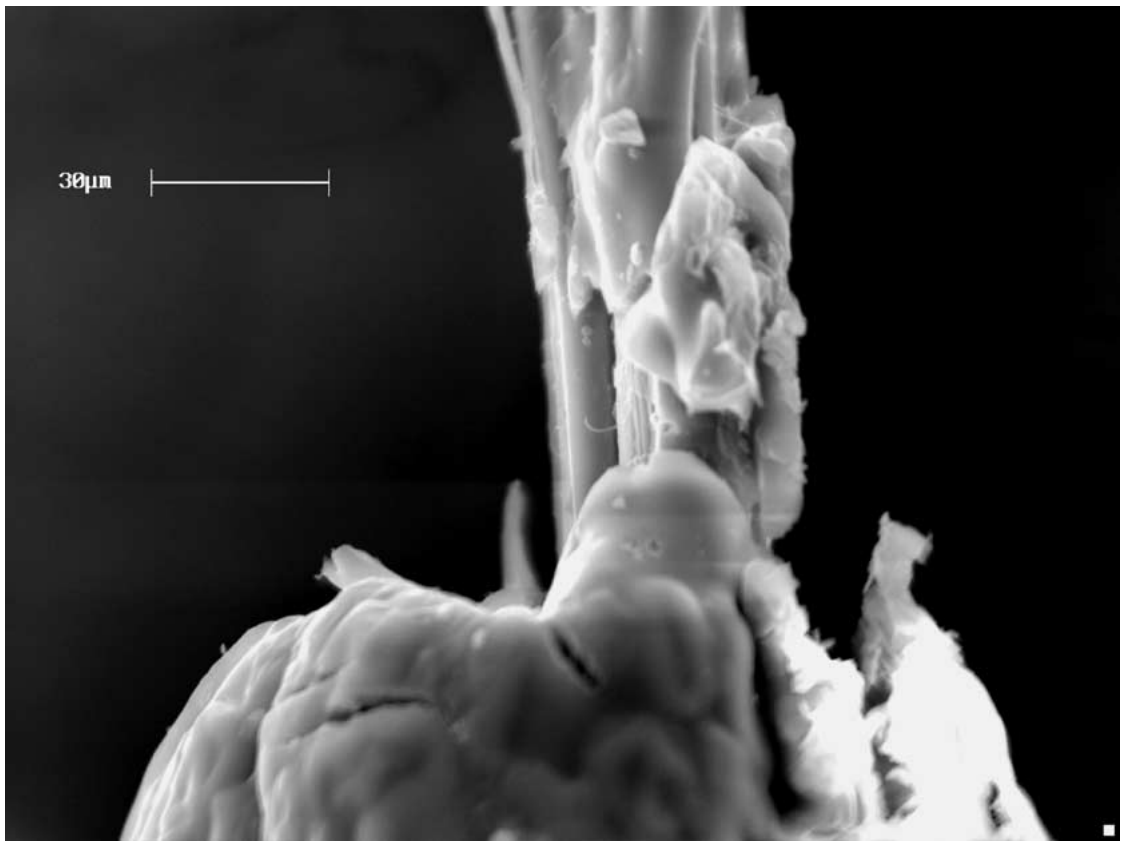


*Figure 5* SEM photomicrograph of the tested microbead on ramie fiber.

### 3.4. Effect of fiber length and content on tensile properties of composites

Figs 6–8 show the plots of fracture stress, Young's modulus, and fracture strain, respectively, of green composites as a function of FWC, for all the three fiber lengths. It can be seen from Fig. 6 that the fracture stress of the composite is lower than the pure SPI polymer for 5 mm fiber length and 10% FWC. Similarly, a decrease in Young's modulus was also observed. The fiber length of 5 mm is close to the critical length of 2.5 mm in

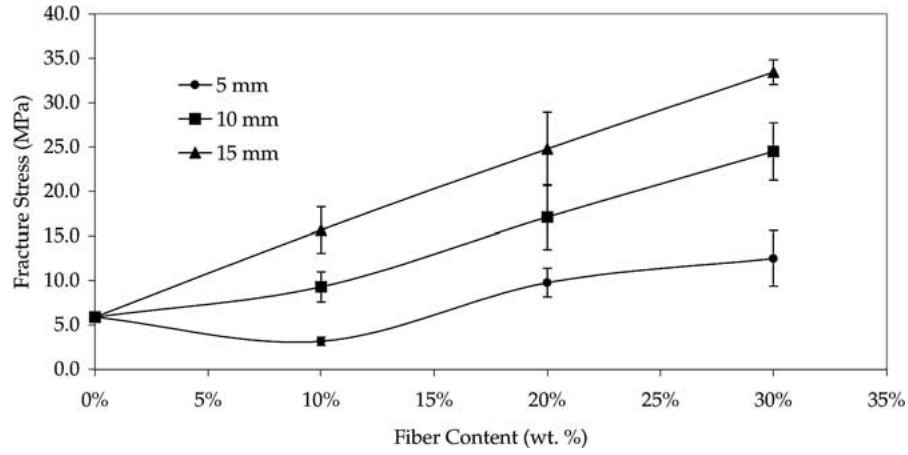


*Figure 6* Effect of fiber content on the fracture stress of ramie fiber reinforced SPI-polymer composite.

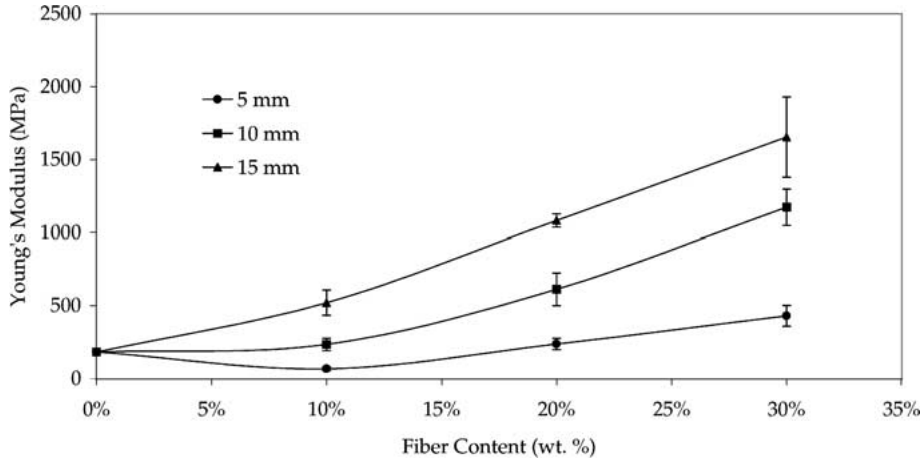


*Figure 7* Effect of fiber content on the Young's modulus of ramie fiber reinforced SPI-polymer composite.

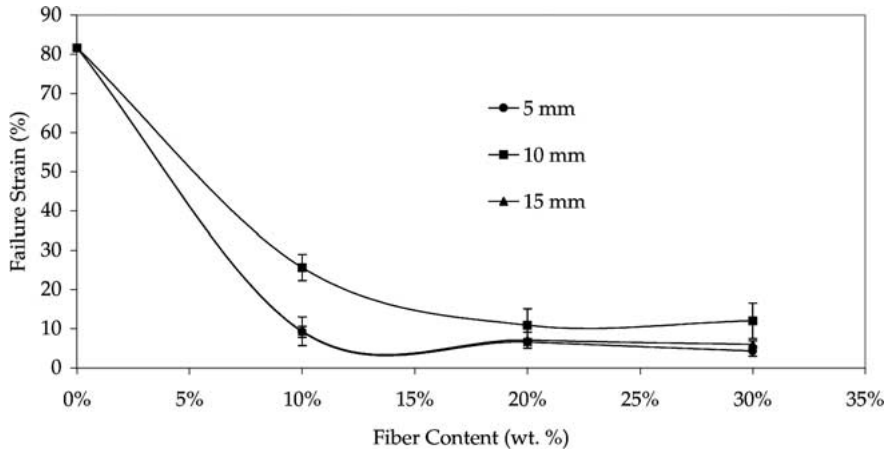


*Figure 8* Effect of fiber content on the fracture strain of ramie fiber reinforced SPI-polymer composite.

absolute value. As a result, the composites with low fiber content of 10% (w/w) do not show any contribution to the fracture stress from fibers. Instead, the fibers with low aspect ratio seem to act like particles, low stress bearing points. Inclusion of short fibers at this low weight content, thus, seems to act as imperfections or flaws to reduce the composite strength. Other reasons are explained later.

With higher fiber content, the fracture stress increases steadily. The trend for Young's modulus as shown in Fig. 7, is also very similar. As expected, the fracture strain (Fig. 8) shows a steady decline from 81.6% to 4.3% as the fiber content increases from 0 to 30%, respectively, and the fibers begin to control the composite fracture strain value. For fibers with 10 and 15 mm length, both strength and modulus values increase with increasing fiber content while the fracture strain decreases, as expected.

As for 10 and 15 mm long fibers, where the length is well above the critical length value, significant reinforcement effect is observed. Longer fibers will have less fiber-ends and hence there would be less flaws or low stress bearing points. Thus, the composite fracture stress and modulus increase and fracture strain

TABLE I Predictions for Young's modulus (GPa) of the composites with various fiber lengths and contents using Zweben's model [31]

| | Fiber weight content | | |
|---|---|---|---|
| Fiber length | 10% | 20% | 30% |
| 5 mm | 0.75 | 1.36 | 1.99 |
| 10 mm | 0.82 | 1.48 | 2.16 |
| 15 mm | 0.85 | 1.52 | 2.21 |

decreases on increasing the fiber length. However, the trend for fracture strain was not evident due to the fiber concentrations at higher fiber lengths and contents. As the fiber content is increased, more fibers are available per unit cross-section area of the composite and hence the fracture stress and modulus increase and the fracture strain decreases. However, for 30% fiber weight content and longer fiber lengths, a large number of specimens showed delamination. As a result, expected strength values for these composites were not achieved. The delaminated surfaces indicate poor wetting of the fibers and also bundling of fibers. With better control in processing, it should be possible to prepare better composites and achieve higher strengths.

The predictions for Young's modulus for composites of various fiber lengths and contents using Zweben's model (based on Cox's approach) are presented in Table I [31]. For all experimental combinations of fiber contents and lengths the experimental Young's modulus values fall short of the theoretical modulus values obtained using Zweben's model [32]. This is believed to be because of the high variability of fiber strength and non-random distribution and orientation of the fibers in the composites. The ramie fibers show a low shape parameter, which implies high variability in terms of fracture stress, which is typical for most plant-based and other natural fibers. Also, various composite specimens prepared in this study showed some fiber-rich and some resin-rich regions as a result of non-uniform fiber distribution. For composites with 10% FWC, the failure occurred in the region where the local fiber content was the lowest, as expected. As a result, the measured fracture stress values of the composites were corresponding to a lower effective fiber content as compared to the intended fiber content. The orientation of the short fibers, however uniformly random in a long-range, usually showed a short-range uneven distribution. Thus the lack of perfect randomness caused some deviations, mostly lower, in expected trend in the tensile properties of the composites. Some other plausible reasons are presented in the subsequent paragraphs.

The Zweben's model assumes an elastic matrix that is perfectly bonded to an elastic fiber [32]. Although, the fiber is elastic, the matrix is not. The matrix shows a large amount of plastic deformation along with the initial elastic deformation similar to polypropylene and polyethylene. The assumption of a perfect interface may also be not met by the ramie/SPI-polymer system because of the presence of unintentional voids. In addition, as mentioned earlier, delaminations were observed in composites with higher FWC indicating poor resin wetting of the fibers. The model also assumes that the fibers have a round cross-section. The ramie fibers, however, are fibrillar in nature and do not have a uniformly circular cross-section, as seen in Fig. 1. Individual fibrils, however, are somewhat oval in cross-section.

The fiber length distribution about the average intended fiber length also contributes towards lower fracture stress as shorter fibers act as poor reinforcements. Shorter fiber lengths also implies higher variation in fiber length. Other factors include presence of some voids in composites, moisture absorption by the matrix/fiber and thermal degradation of the fibers during hot pressing. Many of these factors may be overcome by improving the process for making composites.

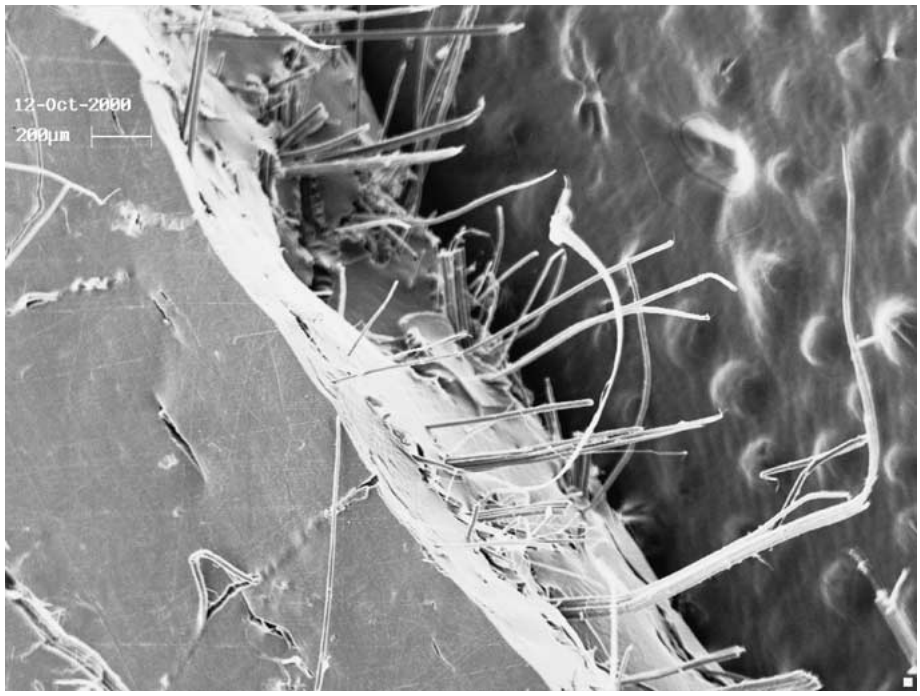


*Figure 9* SEM photomicrograph of fractured surface of composite specimen with 15 mm fiber length and 20% fiber content.


*Figure 10* SEM photomicrograph of fibers just above the fractured surface of composite specimen with 15 mm fiber length and 30% fiber content.

### 3.5. Composite fracture surface analysis

SEM photomicrograph of a typical fracture surface of a composite specimen with 15 mm fiber length and 20% fiber content is shown in Fig. 9. The fracture surfaces show few fibers/fibrils protruding out with transverse fracture, suggesting a brittle failure. Also, the protruding fiber/fibril lengths are short. This confirms good fiber/resin bonding. Fig. 10 shows a SEM photomicrograph of the fibers protruding from the fracture surface of a composite specimen with 15 mm fiber length and 30% fiber content. The photomicrograph had been taken slightly about the fracture surface. A large extent of fiber fibrillation can be seen in these photomicrographs. As seen in Fig. 10, some of these fibrils show resin adhering on the surface whereas some fibrils have a comparatively smoother surface without much resin. The photomicrograph also shows the fractured resin all over the fibers. This indicates that there may be no interfacial debonding at some locations. Since, the IFSS is stronger than the resin shear strength, the debonding may have been caused by voids near the fiber surface. It is also possible that these fibrils may be from the central part of the fibers where it is impossible for the resin to reach.

## 4. Conclusions

This research has shown that the ramie fibers and SPI polymer form a compatible system to give moderate strength composites. However, there is significant scope to improve the tensile properties of both the SPI-polymer and the composites containing natural fibers by modifying processes. Following broad conclusions may be drawn from this study:

1. The ramie fibers showed an average fracture stress of 621 MPa, Young's modulus of 47.5 GPa, fracture strain of 1.9% and energy at break of $7.44 \times 10^{-4}$ J.

2. The SPI-polymer containing 30% glycerol had a density of 1.31 gm/cc after processing. The resin showed an average fracture stress of 5.9 MPa, Young's modulus of 184 MPa and a failure strain of 81.6%. The tensile properties of SPI-polymer resin were found to be highly sensitive to moisture and glycerol content.

3. The ramie fiber/SPI-polymer interface showed an average IFSS of 30 MPa. Based on this IFSS value, the critical length of ramie fibers for SPI-polymer resin was calculated to be 2.54 mm.

4. As expected, the short fiber composites showed increased fracture stress and modulus with increase in both the fiber content and the fiber length. However, for long fiber length of 15 mm and fiber content of 30%, a large amount of delamination was observed. Both fracture stress and Young's modulus were significantly lower than expected due to interlaminar failure.

5. The results for Young's modulus were not found to be in good agreement with the predictions made by Zweben's model for lower fiber contents and lengths but significantly better for higher fiber contents and fiber lengths.

6. The fit of the experimental data to the model could be improved significantly by improving the processing conditions and avoiding voids and uneven fiber distribution in the composites.

## Acknowledgements

We would like to acknowledge the financial support provided by College of Human Ecology, Cornell University, Ithaca, NY for this research. We would also like to acknowledge the support provided by Dr. Yash Kamath, TRI/Princeton, Princeton, NJ for density measurements.

## References

1. The Corporate Units in the Daimler-Benz Group, Daimler-Benz High Tech Report 2, 1995, 1.

2. A. K. MOHANTY, M. MISRA and G. HINRICHSEN, *Macromolecular Materials and Engineering* **276** (2000) 1.
3. K. JOSEPH, S. THOMAS and C. PAVITHRAN, *Polymer* **37** (1996) 5139.
4. J. H. PEDRO and D. J. A. MANUEL, *J. Appl. Polym. Sci.* **65** (1997) 197.
5. J. P. SCHNEIDER and A. C. KARMAKER, *J. Mater. Sci.* **15** (1996) 201.
6. S. LUO and A. N. NETRAVALI, *Polymer Composites* **20** (1999) 367.
7. *Idem.*, *J. Mater. Sci.* **34** (1999) 3709.
8. L. JIANG and G. HINRICHSEN, *Die Angewandte Makromokulare Chemie* **268** (1999) 13.
9. A. K. MOHANTY, M. A. KHAN and G. HINRICHSEN, *Composites: Part* A **31** (2000) 143.
10. R. P. WOOL, S. KOSEFOGLU, R. ZHAO, G. PALMESE and S. KHOT, International Patent Publication No. WO 99/21900, May 6, 1999.
11. J. U. OTAIGBE, H. GOEL, T. BABCOCK and J. JANE, *Journal of Elastomers and Plastics* **31** (1999) 56.
12. I. PAETAU, C. Z. CHEN and J. L. JANE, *Industrial and Engineering Chemistry Research* **33** (1994) 1821.
13. S. F. THAMES and L. ZHOU, in Proceedings of the International Conference on Composites Engineering-5, Las Vegas, July 5–11, 1998, p. 887.
14. F. LIANG, Y. WANG and S. SUN, *Journal of Polymer Engineering* **19** (1999) 383.
15. P. LODHA and A. N. NETRAVALI, in Proceedings of the International Conference on Composites Engineering-7, Denver, July 2–8, 2000, p. 655.
16. *Idem.*, in "Recent Advances in Polymers and Composites," edited by G. N. Mathur, L. D. Kandpal and A. K. Sen (Allied Publishers, New Delhi, India, 2000), p. 3.
17. K. LIU, in "Soybeans-Chemistry, Technology and Utilization" (International Thomson Publishing, Florence, KY, 1997) p. 25, 386, 389, 392.
18. J. C. CHEFTEL, J. L. CUQ and D. LORIENT, in "Food Chemistry," edited by O. R. Fennama (Dekker, New York, 1985), p. 279, 289, 336 and 343.
19. T. E. CREIGHTON, "Proteins: Structure and Molecular Properties," 2nd ed. (Freeman, New York, 1993) p. 1.
20. L. G. ANGELINI, A. LAZZERI, G. LEVITA, D. FONTANELLI and C. BOZZI, *Industrial Crops and Products* **11** (2000) 145.
21. B. W. ROSEN, *Amer. Inst. Aeronaut. Astronaut. (AIAA)* **2** (1964) 1985.
22. P. J. HERRERA-FRANCO and L. T. DRZAL, *Composites* **23** (1992) 2.
23. A. N. NETRAVALI and W. SACHSE, *Polymer Composites* **12** (1991) 370.
24. A. N. NETRAVALI, L. T. T. TOPOLESKI, W. H. SACHSE and S. L. PHOENIX, *Composite Science and Technology* **35** (1989) 13.
25. L. J. BROUTMAN, "Interfaces in Composites," ASTM STP 452 (American Society for Testing and Materials, 1969) p. 27.
26. S. LUO and A. N. NETRAVALI, *Journal of Adhesion Science and Technology* **15** (2001) 423.
27. C. T. CHOU, U. GAUR and B. MILLER, *Journal of Adhesion* **53** (1995) 33.
28. B. MILLER, P. MURI and L. REBENFELD, *Composite Science and Technology* **28** (1987) 17.
29. A. N. NETRAVALI and Z. F. LI, "Polymer and Fiber Science: Recent Advances," edited by R. E. Fornes, R. D. Glibert and H. Mark (VCH Publishers, New York, 1992), ch. 6, p. 67.
30. P. S. MUKHERJEE and K. G. SATYANARAYANA, *J. Mater. Sci.* **21** (1986) 51.
31. P. LODHA, Master of Science-thesis, Cornell University, Ithaca, NY, 2001, p. 45.
32. C. ZWEBEN, H. T. HAHN and T. W. CHOU, in "Mechanical Behavior and Properties of Composite Materials, Delaware Composites Design Encyclopedia," Vol. 1, edited by L. A. Carlsson and J. W. Gillespie (Technomic Publishing, Lancaster, PA, 1989) p. 34.

*Received 8 August 2001*
*and accepted 17 April 2002*